NRL Report 7086

An Iterative Technique for Reducing Sidelobes of Circular and Cylindrical Arrays

H. P. COLEMAN

Microwave Techniques Branch
Electronics Division

June 22, 1970

NAVAL RESEARCH LABORATORY
Washington, D.C.

CONTENTS

ABSTRACT

An iterative technique which allows the computation of low sidelobe current distributions for circular and cylindrical arrays, has been developed and computer implemented. The method is described, and examples are shown of its use in calculating current distributions for circular arrays of 32 axial dipoles with half-wavelength element spacing. For such arrays of $2Q$ elements, azimuth directivities only 0.25 dB less than the directivity of an order-Q Tchebycheff pattern with the same sidelobe level have been obtained.

PROBLEM STATUS

This is an interim report; work continues on other phases of the problem.

AUTHORIZATION

NRL Problem R08-37
Project RR 008-05-41-5700

Manuscript submitted March 3, 1970.

AN ITERATIVE TECHNIQUE FOR REDUCING SIDELOBES OF CIRCULAR AND CYLINDRICAL ARRAYS

INTRODUCTION

Circular and cylindrical arrays of radiating elements can be used to produce beam patterns which may be rotated through 360 degrees by a cyclic permutation of the element currents, making them an attractive choice for numerous applications in radio, radar, and sonar. The successful design of these arrays requires a method for determining the element currents that will yield a desired radiation pattern. A method of approximate synthesis, due to DuHamel (1) is the primary basis for this element current determination. In this method, an exact synthesis for a continuous, cylindrical, current distribution is first derived, and this continuous distribution is then approximated by a finite array of discrete sources on the cylinder. This approach works well if a large number of closely spaced elements is used to approximate the continuous distribution, even for high-resolution, low-sidelobe beam patterns. However, if the method is used to attempt the synthesis of a pattern having nearly optimum resolution for a given sidelobe level, with element spacings of about one-half wavelength, substantial differences may exist between the desired pattern and the performance attained. An iterative method, which progressively improves the sidelobe level of the radiation pattern of such a circular or cylindrical array, has been devised and computer implemented.

DUHAMEL'S SYNTHESIS METHOD

Due to the relative difficulty of obtaining Ref. 1, DuHamel's synthesis method will be summarized here. Attention will be restricted to axial dipole current elements of infinitesimal height, arranged on a circle concentric with a conducting cylinder. The method, however, is equally applicable to other current elements of practical importance: e.g., tangential dipole elements, axial and circumferential slots.

The coordinate system utilized is shown in Fig. 1. The conducting cylinder has a radius of ρ_1 and a continuous current sheet is located concentrically with this cylinder at a radius of ρ_2. The coordinates of a far-field point P are given by φ, θ, and r. Assuming a vertically polarized current sheet whose height is small in terms of wavelength, and with a current distribution of $I(\alpha)$, the electric field intensity at a far field point P due to a current element at (ρ_2, α) and of infinitesimal width $d\alpha$ is given by (2)

$$E_\theta(\varphi, \theta) = K \sin\theta \; I(\alpha) \; \rho_2 \; d\alpha \sum_{n=0}^{\infty} \epsilon_n F_n \cos n(\varphi - \alpha) \;, \tag{1}$$

$$\epsilon_n = \begin{cases} 1 & \text{when } n = 0 \\ 2 & \text{otherwise .} \end{cases}$$

In this equation, K contains the usual dependence on r and the time dependence is understood. For an axial dipole current element in front of a conducting cylinder,

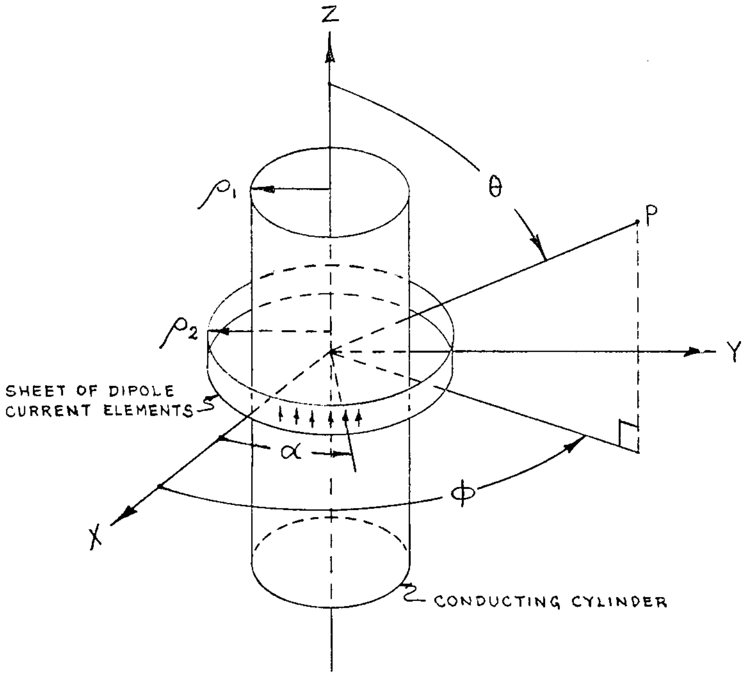

Fig. 1 - Coordinate system

$$F_n = (j)^n \left\{ J_n(\beta\rho_2 \sin\theta) - J_n(\beta\rho_1 \sin\theta) \frac{H_n^{(2)}(\beta\rho_2 \sin\theta)}{H_n^{(2)}(\beta\rho_1 \sin\theta)} \right\} . \tag{2}$$

$H_n^{(2)}$ is a Hankel function of the second kind of order n, and β is the usual $2\pi/\lambda$ ratio.

Rewriting Eq. (1) in complex form yields

$$E_\theta(\varphi,\theta) = K \sin\theta \; I(\alpha) \; \rho_2 \sum_{n=-\infty}^{\infty} F_n(\rho_1,\rho_2,\theta) \; e^{jn(\varphi-\alpha)} \; d\alpha \; . \tag{3}$$

The total field at P is then given immediately by

$$E(\varphi,\theta) = K \sin\theta \; \rho_2 \int_0^{2\pi} I(\alpha) \sum_{n=-\infty}^{\infty} F_n(\rho_1,\rho_2,\theta) \; e^{jn(\varphi-\alpha)} \; d\alpha \; . \tag{4}$$

Expanding $I(\alpha)$ in a complex Fourier series yields

$$I(\alpha) = \sum_{m=-\infty}^{\infty} I_m \, e^{jm\alpha} \; . \tag{5}$$

Substituting from Eq. (5) into Eq. (4) and integrating gives, for the total field at P,

$$E(\varphi,\theta) = 2\pi K \sin\theta \; \rho_2 \sum_{n=-\infty}^{\infty} I_n F_n(\rho_1,\rho_2,\theta)\, e^{jn\varphi} \;, \tag{6}$$

due to the orthogonality of the Fourier terms.

We note that $F_n = F_{-n}$. Then, for a fixed $\theta = \theta_0$,

$$E(\varphi,\theta_0) = 2\pi K \sin\theta_0 \; \rho_2 \sum_{n=0}^{\infty} \epsilon_n I_n F_n(\rho_1,\rho_2,\theta_0) \cos n\varphi \;. \tag{7}$$

A Tchebycheff pattern of order N may be expressed as an exact, finite, Fourier series:

$$T^N(\varphi) = \sum_{n=0}^{N} C_n^N \cos n\varphi \;. \tag{8}$$

The values of C_n^N, of course, depend upon the sidelobe level. Restricting our attention to the synthesis of such a pattern, we may equate the total field to such a pattern. Equating Eqs. (7) and (8) term by term yields, after transposition,

$$I_n = \frac{C_n^N}{\epsilon_n \, 2\pi K \; \sin\theta_0 \; \rho_2 \, F_n(\rho_1,\rho_2,\theta_0)} \quad (n = 0,\ 1,\ \ldots\ N) \;. \tag{9}$$

Due to symmetry, the continuous current distribution required to synthesize the desired pattern may be obtained immediately from Eq. (5), yielding the result

$$I(\alpha) = \sum_{n=0}^{N} \epsilon_n I_n \cos n\alpha \;. \tag{10}$$

Following DuHamel, if we approximate the above continuous distribution by a discrete array of $2Q$ equally spaced current sources, the current on the kth element becomes

$$I(\alpha_k) = \sum_{n=0}^{N} \epsilon_n I_n \cos n\alpha_k \;. \tag{11}$$

The radiation pattern of such an array, for $\theta = \theta_0$, is given by

$$E(\varphi,\theta_0) = K \sin\theta_0 \; \rho_2 \sum_{k=1}^{2Q} I(\alpha_k) \sum_{n=0}^{\infty} \epsilon_n F_n \cos n(\varphi - \alpha_k) \;. \tag{12}$$

DuHamel suggests the use of $2Q$ current sources, arranged at approximately 0.4λ spacing, to approximate the continuous distribution required to synthesize exactly a Tchebycheff pattern of order Q or less. Figure 2 is a plot of beamwidth vs sidelobe level for radiation patterns obtained when this method is applied to an array of 32 axial dipoles, with ρ_1 equal to 2.2965 wavelengths and ρ_2 equal to 2.5465 wavelengths. These radii result in elements a quarter wavelength from the cylinder and a half-wavelength arc length apart. In this figure an abbreviated notation is used; $T^N(p)$ indicates an exact Tchebycheff with order N with sidelobes of p dB, whereas $T^N(\bar{p})$ denotes the result of the above method of approximate synthesis. It is to be noted that substantial errors exist in

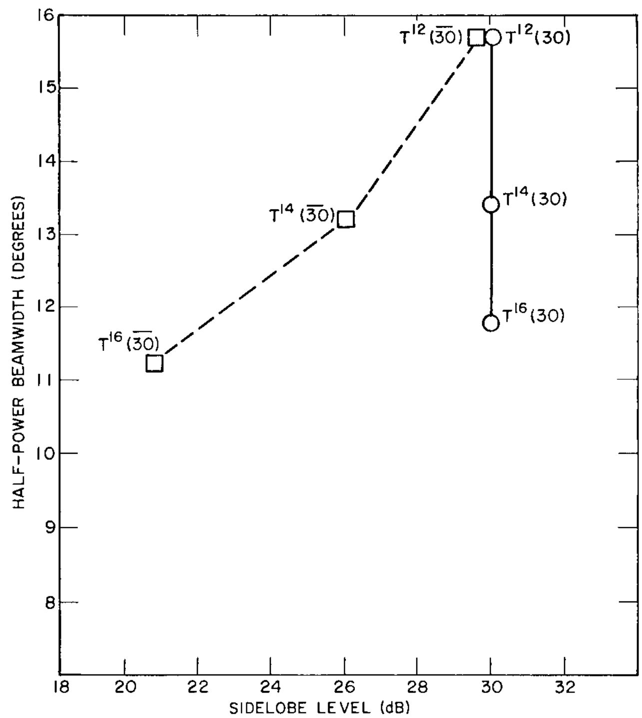

Fig. 2 - Beamwidth vs sidelobe level for current distributions on a circular array of dipole current elements

the approximate synthesis procedure as N approaches Q. The iterative technique described in this report improves upon this approximate synthesis under these conditions.

THE ITERATIVE METHOD

As an example of the use of the iterative method, results are shown for the attempted synthesis of a Tchebycheff pattern of order 16 with 30-dB sidelobes. This pattern is taken as the objective pattern, in the principal plane, of the circular array of 32 dipoles equally spaced around a conducting cylinder with a radius of 2.2965 wavelengths. As before, the dipoles are arranged on a circle of 2.5465-wavelength radius. In Figure 3, the objective pattern and the pattern resulting from using DuHamel's approximate synthesis for this array are plotted. The interval of computation is 2 degrees, and both patterns are symmetric about 0 degrees. A Tchebycheff pattern of order Q has $2Q$ maxima. It is to be noted that, although the approximate synthesized pattern has sidelobes as high as -20.8 dB, it still has the characteristic 32 maxima. The essential feature of the developed iterative technique is the numerical determination of the positions of these maxima and the solution of a system of simultaneous equations which impose constraints on the pattern at these positions. Provision is made in the computer algorithm for substituting pairs of symmetrically located constraints on the main beam for missing positions of maxima, in the event that less than $2Q$ maxima exist.

From Eq. (1) the principal plane far-field pattern of a circular array of $2Q$ current elements arranged around a perfectly conducting cylinder may be written in the form

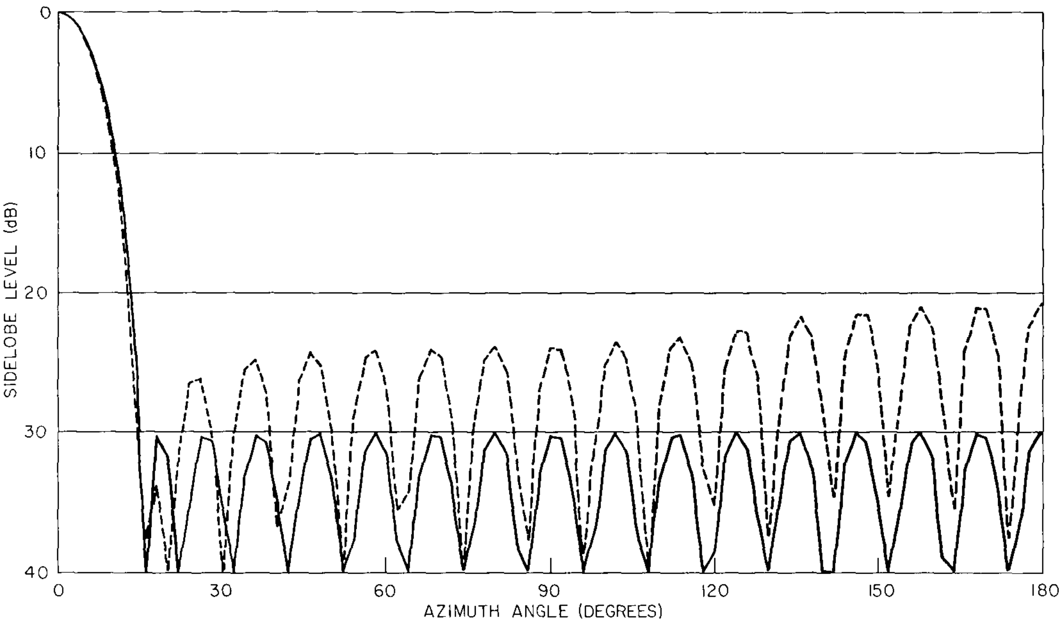

Fig. 3 - $T^{16}(30)$ and $T^{16}(\overline{30})$ radiation patterns

$$E(\varphi) = \sum_{k=1}^{2Q} I_k \sum_{n=0}^{\infty} G_n \cos n(\varphi - \alpha_k) \ . \tag{13}$$

Here, $E(\varphi)$ is proportional to the total E field at the angle φ. The current on the kth element (located on the circle at an angle α_k) is I_k. The set of I_k is normalized so that E is real and equal to 1 at the peak of the main beam. The coefficients G_n depend only on the dimensions of the array, in terms of wavelength, and on the type of current element.

In the present technique, Eq. (1) is used to determine numerically the $2Q$ positions of maxima in the far-field radiation pattern. The expression for the value of the pattern function at these $2Q$ positions then becomes

$$E_j = E(\overline{\varphi}_j) = \sum_{k=1}^{2Q} I_k \sum_{n=0}^{\infty} G_n \cos n(\overline{\varphi}_j - \alpha_k) \tag{14}$$

$$j = 1, 2, \ldots, 2Q \ ,$$

where the positions of maxima are represented by the set of $\overline{\varphi}_j$. Making the substitution

$$A_{jk} = \sum_{n=0}^{\infty} G_n \cos n(\overline{\varphi} - \alpha_k) \tag{15}$$

$$\begin{cases} j = 1, 2, \ldots, 2Q \\ k = 1, 2, \ldots, 2Q \end{cases}$$

yields the set of equations

$$E_j = \sum_k I_k A_{jk} . \tag{16}$$

The range of j and k in this and subsequent equations is the same as in Eq. (15).

We next consider a set of perturbations Λ_k applied to the original set of currents I_k. These perturbations result in new values of E_j, redesignated $\widetilde{E}_j$, for the $2Q$ far-field positions corresponding to the maxima of the original pattern:

$$\widetilde{E}_j = \sum_k (I_k + \Lambda_k) A_{jk} . \tag{17}$$

Substituting from Eq. (16) and transposing results in the set of $2Q$ equations in $2Q$ unknowns

$$\sum_k \Lambda_k A_{jk} = E_j - \widetilde{E}_j . \tag{18}$$

The values of E_j are known from Eq. (16); the $2K$ values of $\widetilde{E}_j$ may be arbitrarily chosen and this set of equations solved for the $2Q$ perturbations of the element currents.

As currently implemented, the far-field magnitude is set equal to its previous value at the main-beam maximum and at the $2Q - 1$ sidelobe positions, a new level, in general lower than in the previous pattern and equal at all sidelobe positions, is chosen. Far-field phase is currently established as a strict 180-degree alternation between adjacent lobes, starting with 0 phase for the main beam. By substituting the perturbed currents for the element currents in Eq. (13) and repeating the above procedure a number of times, an iterative method for sidelobe reduction results.

Current distributions yielding far-field patterns with sidelobe levels equal to and also below the levels of the original objective function (in the example, a Tchebycheff pattern of order 16 with 30-dB sidelobes) have been attained for the cases examined to date. In the example, sidelobes were initially reduced to 24 dB and subsequently reduced in 1-dB increments. Figure 4 shows typical results for this array; intermediate sidelobe reduction steps and an ultimate reduction to 33 dB (i.e., 3 dB below the original objective function) are shown.

For a given sidelobe level, the current distributions obtained by using the above method are not unique, but depend, for instance, on the choice of starting current distribution. By utilizing the method, an entire family of current distributions, resulting in patterns with equal sidelobe levels but differing in detail, may be generated.

ADDITIONAL RESULTS

Figure 5 presents plots of half-power beamwidth vs sidelobe level. The same notation is used as in Fig. 2. In this figure, and also in Fig. 2, all beamwidth data were obtained by linear interpolation in calculated tables of voltage vs far-field angle. Two separate iterative paths are plotted. The path starting with $T^{16}(\overline{30})$ has been discussed above; the path starting with $T^{16}(\overline{20})$ results from an initial sidelobe leveling to 16 dB and subsequent sidelobe reduction in 1-dB increments. At each iterative step the pattern was calculated in 3-degree increments of far-field angle. The best sidelobe level obtained was, in this case, 29 dB; i.e., 9 dB below the original objective level.

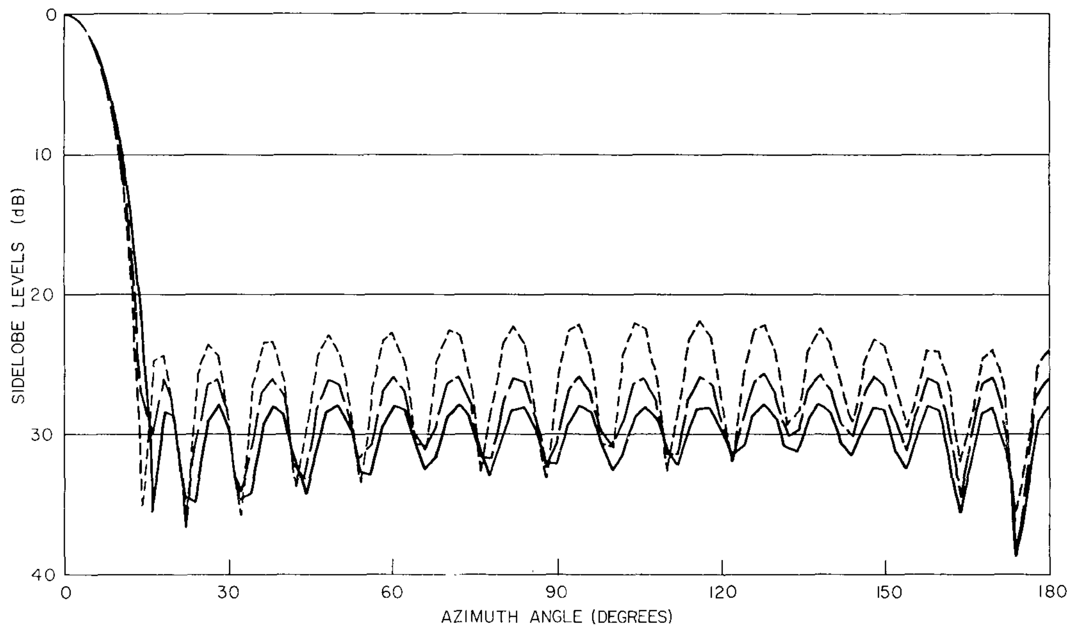

(a)

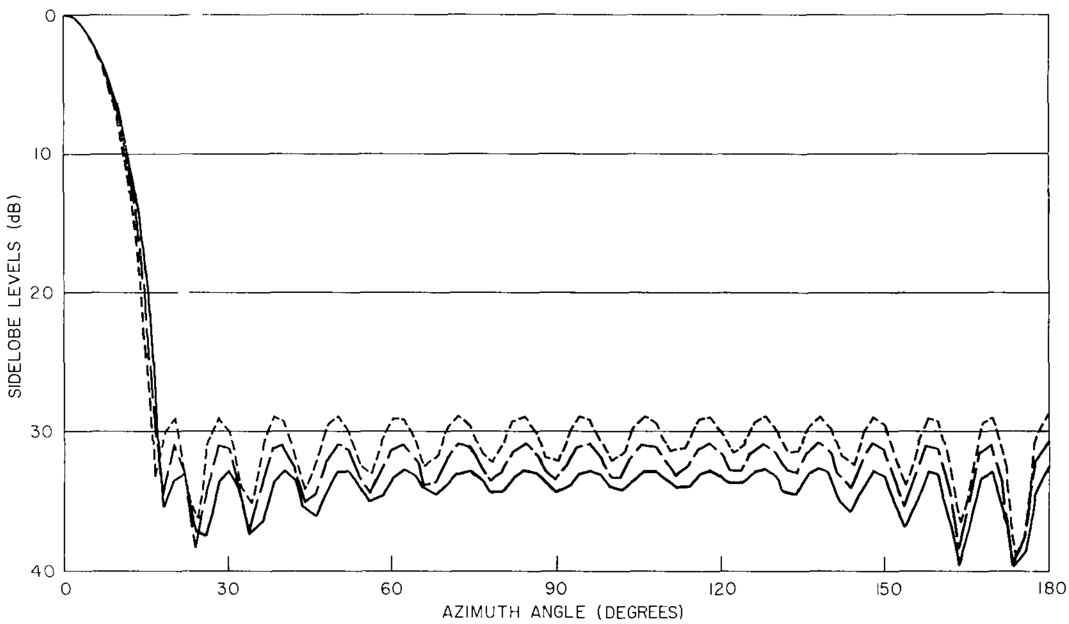

(b)

Fig. 4 - Radiation patterns showing progressive improvement in sidelobe level

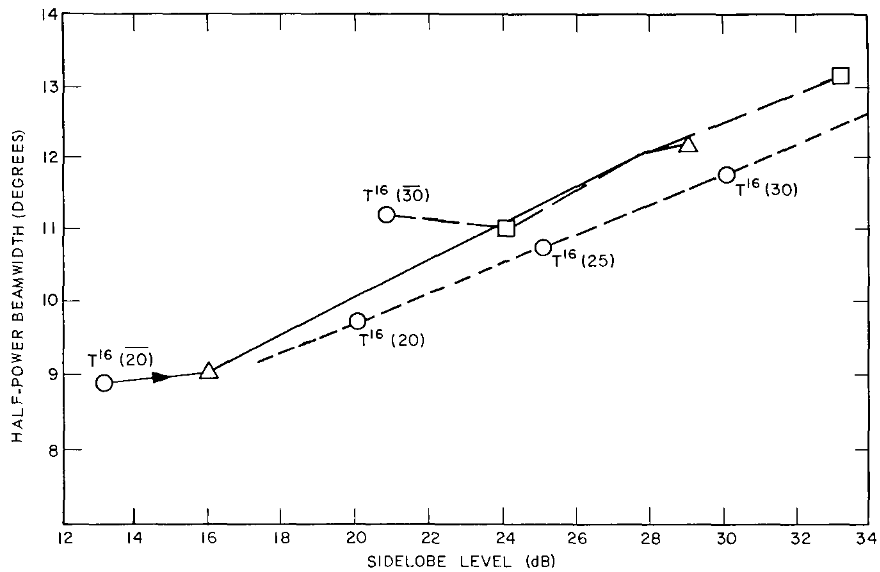

Fig. 5 - Comparison of beamwidth vs sidelobe level plots obtained from iterations with those obtained from ideal Tchebycheff patterns

Figure 5 also includes plotted values for $T^{16}(20)$, $T^{16}(25)$, and $T^{16}(30)$; these plotted data allow comparison of the azimuth resolution of the patterns obtained from the current distributions on discrete arrays, obtained by the iterative technique, with the resolution of the exact Tchebycheff patterns of order 16 having corresponding sidelobe levels. It is interesting to note that only approximately 0.25 dB less directivity is obtained from the derived discrete current distributions than from the corresponding exact Tchebycheff pattern.

The iterative procedure starting with $T^{16}(20)$ was terminated at the 29-dB sidelobe level because, due to the relatively coarse computation interval, an apparent shoulder rather than a maximum appears adjacent to the main beam. Due to the method of assigning far-field phase currently implemented, this causes a reassignment of the far-field phase at all determined positions of sidelobes, the new values differing by exactly 180 degrees from the previous values. This requirement of drastic change in the far-field pattern, of course, destroys the perturbational method. The iterative procedure starting with $T^{16}(30)$ was terminated, rather arbitrarily, at the 33-dB sidelobe level. Beyond the 33-dB level, although the general sidelobe level continued to decrease, occasional lobes higher in amplitude than the assigned objective level appear; and, in general, the positions of maxima begin to change rapidly from one iterative step to the next. This effect is thought to stem from loss of accuracy in the solution of the set of simultaneous equations; this conjecture, however, has not yet been verified.

Figure 6 gives representative plots of the magnitudes of the sets of element currents obtained during the iteration starting with $T^{16}(\overline{30})$, whereas Fig. 7 presents the corresponding phase data. Figures 8 and 9 correspond to Figs. 6 and 7 but are for the iteration discussed which started with $T^{16}(\overline{30})$. In all cases,

$$\alpha_k = (k-1)\,\frac{2\pi}{32}\;; \tag{19}$$

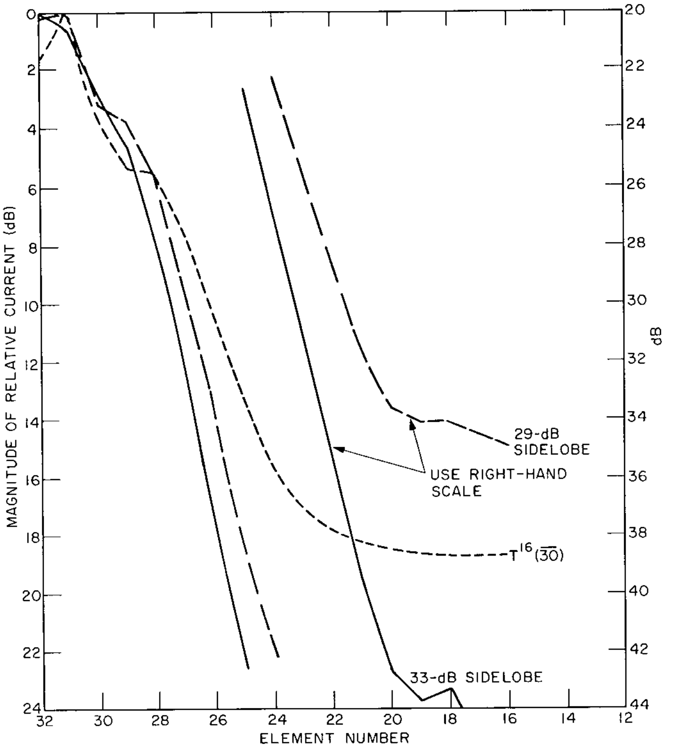

Fig. 6 - Magnitudes of element currents, $T^{16}(\overline{30})$ iteration

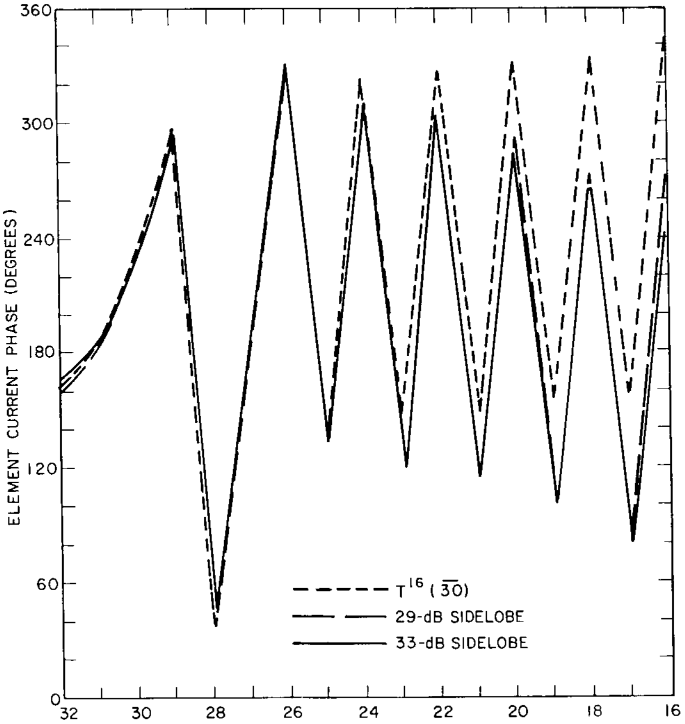

Fig. 7 - Phases of element currents, $T^{16}(\overline{30})$ iteration

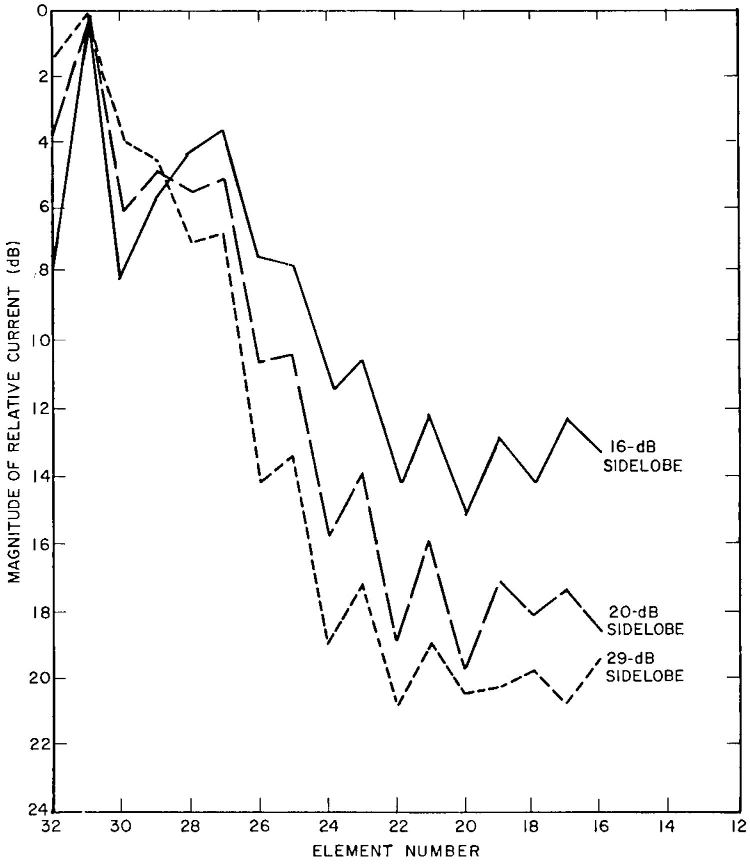

Fig. 8 - Magnitudes of element currents, $T^{16}(\overline{20})$ iteration

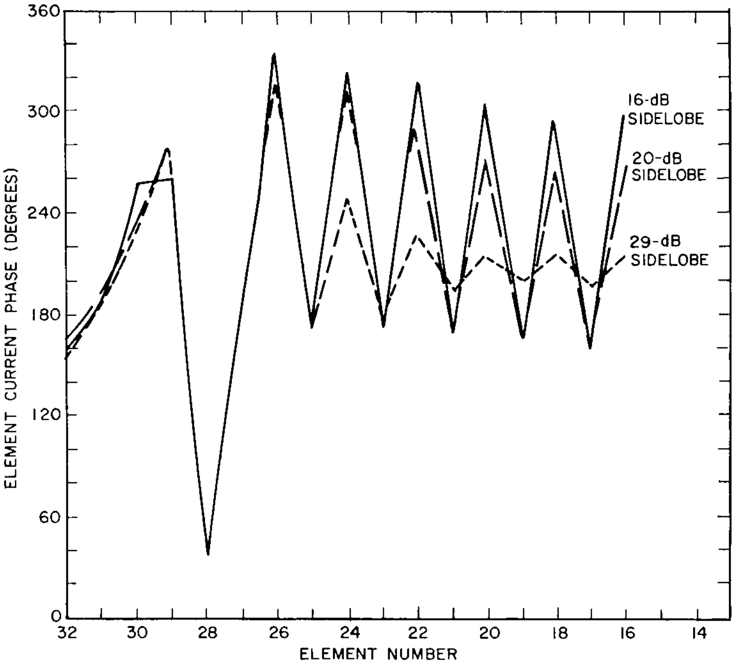

Fig. 9 - Phases of element currents, $T^{16}(\overline{20})$ iteration

i.e., element 32 lies at $\alpha = 0$, and this also corresponds with $\varphi = 0$. The plots are, therefore, for one-half of the array. The difference in phase, for the two cases, on the rearward elements is noteworthy as is the general smoothing of the current distribution with the lowering of the amplitudes on the rearward elements as the iteration proceeds. This effect is most pronounced in Fig. 6.

The data for the $T^{16}(\overline{30})$ iteration indicates that some of the rearward elements might be eliminated, since the magnitude of the currents is quite low on this section of the array. In some applications, this would be highly desirable, and we expect to investigate this possibility in future work.

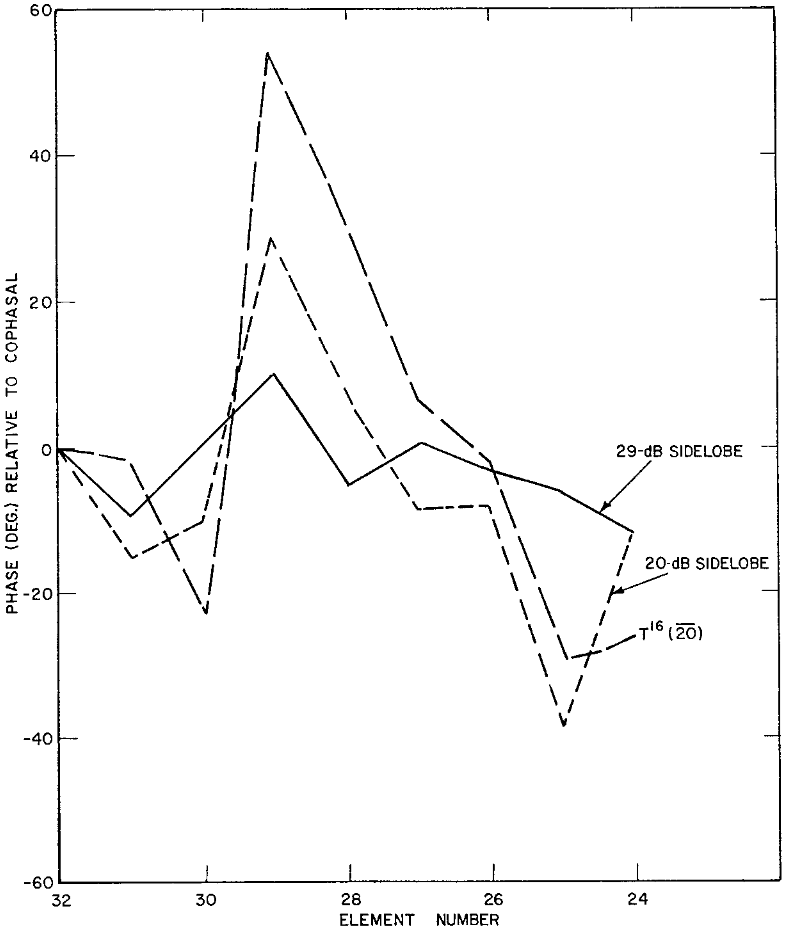

Fig. 10 - Comparison of phases on currents for $T^{16}(\overline{20})$ iteration with a cophasal distribution

In arrays which are composed of sectors of regularly spaced circular arrays, cophasal distributions are frequently used; i.e., distributions in which the elements are phased to a line tangent to the circular sector. Figure 10 compares the phases of elements, for several steps in the $T^{16}(\overline{20})$ iteration, with the phases in cophasal distribution assuming the center of phase of the radiation to be located at

$$\rho_1 + \frac{(\rho_2 - \rho_1)}{3} . \tag{20}$$

Only the phases of currents on the forward half of the array are considered. The data indicate that the phase distribution becomes more nearly cophasal as the sidelobe level is improved. Similar results were obtained for the $T^{16}(\overline{30})$ iteration.

CONCLUSION

An iterative technique has been presented which is capable of deriving low sidelobe current distributions for circular or cylindrical arrays of elements. Examples have been given of the use of this technique for the suppression of sidelobes in the principal plane patterns of two circular arrays of 32 dipole elements, spaced a half-wavelength apart around a conducting cylinder. In one case a current distribution yielding 29-dB sidelobes was obtained; in the other case 33-dB sidelobe patterns were obtained. Both of these patterns, as in other examples of arrays of $2Q$ elements considered to date, exhibit azimuthal directivity only about 0.25 dB less than the order Q Tchebycheff pattern with the same sidelobe level.

REFERENCES

1. DuHamel, R., "Pattern Synthesis for Antenna Arrays on Circular, Elliptical, and Spherical Surfaces," University of Illinois Electrical Engineering Research Technical Report No. 16, pp. 27-59, Urbana, Ill., May 1952

2. Carter, P.S., "Antenna Arrays Around Cylinders," Proc. IRE, 31 (No. 12):671-693 (Dec. 1943)

☆ U.S. GOVERNMENT PRINTING OFFICE: 1970-397-177/223

Security Classification

DOCUMENT CONTROL DATA - R & D

(Security classification of title, body of abstract and indexing annotation must be entered when the overall report is classified)

1. ORIGINATING ACTIVITY *(Corporate author)* Naval Research Laboratory Washington, D.C. 20390	2a. REPORT SECURITY CLASSIFICATION Unclassified	
	2b. GROUP	
3. REPORT TITLE AN ITERATIVE TECHNIQUE FOR REDUCING SIDELOBES OF CIRCULAR AND CYLINDRICAL ARRAYS		
4. DESCRIPTIVE NOTES *(Type of report and inclusive dates)* An interim report on one phase of the problem.		
5. AUTHOR(S) *(First name, middle initial, last name)* H. P. Coleman		
6. REPORT DATE June 22, 1970	7a. TOTAL NO. OF PAGES 16	7b. NO. OF REFS 2
8a. CONTRACT OR GRANT NO. NRL Problem R08-37 b. PROJECT NO. Project RR 008-05-41-5700 c. d.	9a. ORIGINATOR'S REPORT NUMBER(S) NRL Report 7086 9b. OTHER REPORT NO(S) *(Any other numbers that may be assigned this report)*	
10. DISTRIBUTION STATEMENT This document has been approved for public release and sale; its distribution is unlimited.		
11. SUPPLEMENTARY NOTES	12. SPONSORING MILITARY ACTIVITY Department of the Navy (Office of Naval Research), Washington, D.C. 20360	

13. ABSTRACT

An iterative technique which allows the computation of low sidelobe current distributions for circular and cylindrical arrays, has been developed and computer implemented. The method is described, and examples are shown of its use in calculating current distributions for circular arrays of 32 axial dipoles with half-wavelength element spacing. For such arrays of $2Q$ elements azimuth directivities only 0.5 dB less than the directivity of an order-Q Tcheby-cheff pattern with the same sidelobe level have been obtained.

DD FORM 1 NOV 65 1473 (PAGE 1)

S/N 0101-807-6801

Security Classification

14. KEY WORDS	LINK A		LINK B		LINK C	
	ROLE	WT	ROLE	WT	ROLE	WT
Radar Sidelobe suppression for circular and cylindrical arrays						